

Electronic Supporting Information

Cationic mono and dicarbonyl pincer complexes of rhodium and iridium to assess the donor properties of PC_{carbene}P ligands.

Joel D. Smith, Jessamyn R. Logan, Lauren E. Doyle, Richard J. Burford, Shun Sugawara, Chiho Ohnita, Yohsuke Yamamoto, Warren E. Piers*, Denis M. Spasyuk and Javier Borau-Garcia.

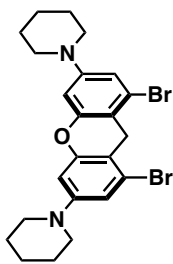
University of Calgary, Department of Chemistry, 2500 University Drive N.W., Calgary, Alberta,
Canada, T2N 1N4

Table of Contents

| | |
|---|-----|
| General Considerations. | S3 |
| Synthesis of 1,1'-(1,8-dibromo-9H-xanthene-3,6-diyl)dipiperidine | S4 |
| Synthesis of 1,1'-(1,8-bis(diisopropylphosphino)-9H-xanthene-3,6-diyl)dipiperidine | S4 |
| Synthesis of 5-Cl | S5 |
| Figure S1. ^1H and $^{13}\text{C}\{\text{H}\}$ spectra of 1,1'-(1,8-dibromo-9H-xanthene-3,6-diyl)dipiperidine in C_6D_6 . | S6 |
| Figure S2. ^1H , $^{13}\text{C}\{\text{H}\}$, $^{31}\text{P}\{\text{H}\}$ NMR spectra of 1,1'-(1,8-bis(diisopropylphosphino)-9H-xanthene-3,6-diyl)dipiperidine in C_6D_6 . | S7 |
| Figure S3. ^1H , $^{13}\text{C}\{\text{H}\}$, $^{31}\text{P}\{\text{H}\}$ NMR spectra of 1-CO in CD_2Cl_2 . | S8 |
| Figure S4. ^1H , $^{13}\text{C}\{\text{H}\}$, $^{31}\text{P}\{\text{H}\}$ NMR spectra of 2-iPr-(CO)₂ in CD_2Cl_2 . | S9 |
| Figure S5. ^1H , $^{13}\text{C}\{\text{H}\}$, $^{31}\text{P}\{\text{H}\}$ NMR spectra of 2-iPr-CO in CD_2Cl_2 . | S10 |
| Figure S6. ^1H , $^{13}\text{C}\{\text{H}\}$, $^{31}\text{P}\{\text{H}\}$ NMR spectra of 2-tBu-(CO)₂ in CD_2Cl_2 . | S11 |
| Figure S7. ^1H , $^{13}\text{C}\{\text{H}\}$, $^{31}\text{P}\{\text{H}\}$ NMR spectra of 2-tBu-CO in CD_2Cl_2 . | S12 |
| Figure S8. ^1H , $^{13}\text{C}\{\text{H}\}$, $^{31}\text{P}\{\text{H}\}$ NMR spectra of 3-(CO)₂ in CD_2Cl_2 . | S13 |
| Figure S9. ^1H , $^{13}\text{C}\{\text{H}\}$, $^{31}\text{P}\{\text{H}\}$ NMR spectra of 3-CO in CD_2Cl_2 . | S14 |
| Figure S10. ^1H , $^{13}\text{C}\{\text{H}\}$, $^{31}\text{P}\{\text{H}\}$ NMR spectra of 4-(CO)₂ in CD_2Cl_2 . | S15 |
| Figure S11. ^1H , $^{13}\text{C}\{\text{H}\}$, $^{31}\text{P}\{\text{H}\}$ NMR spectra of 4-(CO)₂ in CD_2Cl_2 . | S16 |
| Figure S12. ^1H , $^{13}\text{C}\{\text{H}\}$, $^{31}\text{P}\{\text{H}\}$ NMR spectra of 5-Cl in CD_2Cl_2 . | S17 |
| Figure S13. ^1H , $^{13}\text{C}\{\text{H}\}$, $^{31}\text{P}\{\text{H}\}$ NMR spectra of 5-(CO)₂ in CD_2Cl_2 . | S18 |
| Figure S14. ^1H , $^{13}\text{C}\{\text{H}\}$, $^{31}\text{P}\{\text{H}\}$ NMR spectra of 5-CO in CD_2Cl_2 . | S19 |

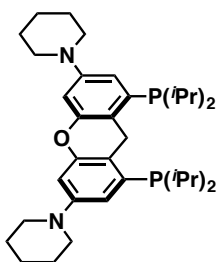
| | |
|--|------------|
| Figure S15. ^1H , $^{13}\text{C} \{^1\text{H}\}$, $^{31}\text{P} \{^1\text{H}\}$ NMR spectra of 6-Cl in CD_2Cl_2 . | S20 |
| Figure S16. ^1H , $^{13}\text{C} \{^1\text{H}\}$, $^{31}\text{P} \{^1\text{H}\}$ NMR spectra of 6-CO in CD_2Cl_2 . | S21 |
| Figure S17. X-Ray structure of 5-Cl . | S22 |
| Figure S18. X-Ray structure of 6-Cl . | S23 |
| Table S1. Iridium (I) monocarbonyl cations supported by pincer ligands | S24 |
| Table S2. Data collection and structure refinement details for 1-CO , iPr-2-(CO)₂ and 3-CO . | S26 |
| Table S3. Data collection and structure refinement details for 4-CO , 5-Cl , 6-Cl and 6-CO . | S27 |
| References | S27 |

General Considerations. Storage and manipulation of all compounds were performed under an argon atmosphere either in a VAC glove box or using a double manifold high vacuum line using standard techniques. Passage of argon through an OxisorBW scrubber (Matheson Gas Products) removed any residual oxygen and moisture. Toluene and tetrahydrofuran were dried and purified using a Grubbs/Dow solvent purification system and stored in 500 mL thick-walled glass pressure flasks over sodium/benzophenone ketal. *n*-Pentane was purified using a M-Braun solvent purification system, dried over sodium/benzophenone ketal and stored in a 100 mL thick-walled glass pressure flask. Benzene-*d*₆ was dried over sodium/benzophenone ketal and stored in a 100 mL thick-walled glass pressure flask. Dichloromethane-*d*₂ was dried over CaH₂ and stored in a 50 mL thick-walled glass pressure flask. All dried solvents were degassed and vacuum distilled prior to use. ¹H and ¹³C NMR chemical shifts were referenced to residual solvent protons and naturally abundant ¹³C resonances for all deuterated solvents. Chemical shift assignments are based on ¹H, ³¹P{¹H}, ¹³C{¹H}, ¹H-¹H-COSY, ¹H-¹³C-HSQC and ¹H-¹³C-HMBC NMR experiments performed on Avance III 400, Ascend-500, or Avance-600 MHz spectrometers. X-ray crystallographic analyses were performed on a Nonius system equipped with a Bruker Apex-II CCD using samples coated in Paratone 8277 oil (Exxon) and mounted on a glass fibre. Full crystallography details can be found in independently uploaded .cif files (CCDC numbers 1485351-1485357). Carbon monoxide gas (>99.0%) was purchased from Sigma-Aldrich and used without further purification. Iridium (III) chloride hydrate was purchased from Pressure Chemicals Inc. and used as received. [Ir(CO)₂(Cl)]₂¹, 1,8-dibromo-3,6-di(piperidin-1-yl)-9*H*-xanthen-9-one² and sodium tetrakis[3,5-bis(trifluoromethyl)phenyl]borate³ were prepared by literature methods. All other reagents were purchased from Sigma-Aldrich and used as received. Elemental and mass spectrometric analyses were performed by staff at the Instrumentation Facility in the Department of Chemistry, University of Calgary.



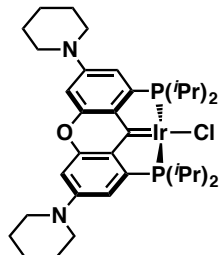
Synthesis of 1,1'-(1,8-dibromo-9H-xanthene-3,6-diyl)dipiperidine – To a thick walled glass pressure flask charged with 1,8-dibromo-3,6-di(piperidin-1-yl)-9H-xanthen-9-one (0.980 g, 1.88 mmol) and a Teflon stirbar, toluene (10 mL) was added followed by PhSiH₃ (0.698 mL, 0.613 g, 5.66 mmol). In a separate vial B(C₆F₅)₃ (0.025 g, 0.047 mmol) was dissolved in toluene (1 mL). The B(C₆F₅)₃ solution was then added dropwise at room temperature over a period of 5 minutes to the mixture in the flask while stirring. The flask was sealed and heated to 45°C for 18 hours. Toluene was removed *in vacuo* and the remaining red solid was washed with Et₂O (3 x 5 mL). The red filtrate was cooled to -20 °C to precipitate any dissolved product. The precipitated product was washed again with cold Et₂O (3 x 2 mL). A white solid was acquired in 70% yield (0.634 g, 1.31 mmol).

¹H NMR (500 MHz, C₆D₆) δ 6.91 (d, ⁴J_{HH} = 2.5 Hz, 2H, ArH), 6.60 (d, ⁴J_{HH} = 2.5 Hz, 2H, ArH), 3.99 (s, 2H, -CH₂-), 2.73 (m, 8H, -N(CH₂)₅), 1.29 (m, 8H, -N(CH₂)₅), 1.20 (m, 4H, -N(CH₂)₅). ¹³C NMR (126 MHz, C₆D₆) δ 152.9 (s, ArC), 152.6 (s, ArC), 125.8 (s, ArC), 115.2 (s, ArCH), 111.0 (s, ArC), 102.9 (s, ArCH), 49.8 (s, -N(CH₂)₅), 29.9 (s, -CH₂-), 25.7 (s, -N(CH₂)₅), 24.4 (s, -N(CH₂)₅). Elemental Anal. Calcd. (%) for C₂₃H₂₆Br₂N₂O: C 54.56; H 5.18; N 5.53. Found: C 54.60; H 5.14; N 5.49.



Synthesis of 1,1'-(1,8-bis(diisopropylphosphino)-9H-xanthene-3,6-diyl)dipiperidine – To a two-necked round bottom flask charged with 1,1'-(1,8-dibromo-9H-xanthene-3,6-diyl)dipiperidine (0.192 g, 0.379 mmol) and a Teflon stirbar, THF (10 mL) was vacuum transferred at -78°C. The mixture was stirred and kept at -78°C while ^tBuLi (1.7 M, 0.90 mL, 1.517 mmol) was added dropwise over a period of 15 minutes. After stirring for 2 hours at -78°C, chlorodiisopropylphosphine (0.120 mL, 0.758 mmol) was added to the flask. The mixture was slowly warmed to room temperature and stirred for 18 hours. THF was removed *in vacuo* and the remaining mixture was washed with hexanes (3 x 5 mL). The hexanes filtrate was collected and the solvent was removed *in vacuo* to give a white solid in 77% yield (0.170g, 0.293 mmol). Further purification could be achieved through recrystallization under an argon atmosphere using hot pentane.

¹H NMR (500 MHz, C₆D₆) δ 6.97 (dd, ⁴J_{HH} = 2.5 Hz, 2H, ArH), 6.94 (d, ⁴J_{HH} = 2.5 Hz, 2H, ArH), 4.93 (t, ⁴J_{HP} = 2.6 Hz, 2H, Ar-CH₂-Ar), 3.02 (m, 8H, -N(CH₂)₅), 2.05 (d sept, ²J_{HP} = 1.0 Hz, ³J_{HH} = 6.9 Hz, 4H, -CH(CH₃)₂), 1.49 (m, 8H, -N(CH₂)₅), 1.30 (m, 4H, -N(CH₂)₅), 1.15 (dd, ³J_{HH} = 6.9, ³J_{HP} = 14.8 Hz, 12H, -CH(CH₃)₂), 1.01 (dd, ³J_{HH} = 6.9, ³J_{HP} = 11.4 Hz, 12H, -CH(CH₃)₂). ¹³C{¹H} NMR (126 MHz, C₆D₆) δ 154.0 (d, ³J_{CP} = 9.2 Hz, ArC), 151.7 (s, ArC), 135.6 (d, ¹J_{CP} = 22.0 Hz, ArC), 120.4 (dd, ⁴J_{CP} = 4.3 Hz, ²J_{CP} = 28.0, ArC) 117.0 (s, ArCH), 106.0 (s, ArCH), 51.3 (s, -N(CH₂)₅), 28.0 (t, ³J_{CP} = 27.5 Hz Ar-CH₂-Ar), 26.1 (s, -N(CH₂)₅), 24.7 (s, -N(CH₂)₅), 24.5 (d, ²J_{CP} = 14.4 Hz, -CH(CH₃)₂), 20.5 (d, ²J_{CP} = 19.5 Hz, -CH(CH₃)₂), 19.6 (d, ²J_{CP} = 10.4 Hz, -CH(CH₃)₂). ³¹P{¹H} NMR (203 MHz, C₆D₆) δ -6.4 (br s). Elemental Anal. Calcd. (%) for C₃₅H₅₄N₂OP₂: C 72.38; H 9.37; N 4.82. Found: C 72.45; H 9.13; N 4.60.



Synthesis of 5-Cl – To a thick walled glass pressure flask (25 mL) charged with 1,1'-(1,8-bis(diisopropylphosphino)-9H-xanthene-3,6-diyl)dipiperidine (0.186 g, 0.320 mmol), [Ir(COEt)₂(Cl)]₂ (0.144 g, 0.161 mmol) and a Teflon stirbar, toluene (10 mL) was added. The flask was sealed and the solution was stirred at 100 °C for 4 hours. The flask was cooled to room temperature and the solution was filtered through a sintered glass funnel. The filtrate was collected and the toluene was removed *in vacuo* under high vacuum. The collected solid was washed with *n*-pentane (3 x 2 mL). A dark brown solid was isolated in 75% yield (0.194 g, 0.241 mmol). X-ray quality crystals were obtained through slow evaporation of a saturated solution of **5-Cl** in *n*-pentane.

¹H NMR (500 MHz, C₆D₆) δ 6.89 (dvt, ⁴J_{HH} = 2.0 Hz, ³J_{HP} = 3.4 Hz 2H, ArH), 6.25 (d, ⁴J_{HH} = 2.0 Hz, 2H ArH), 3.07 (septvt, ³J_{HH} = 7.0 Hz, ²J_{HP} = 2.1 Hz, 4H, -CH(CH₃)₂), 2.76-2.72 (m, 8H, N(CH₂)₅), 1.68 (dvt, ³J_{HH} = 7.8 Hz, ³J_{HP} = 7.6 Hz, 12H, -CH(CH₃)₂), 1.33 (d, ³J = 7.0 Hz, 12H, -CH(CH₃)₂), 1.32-1.38 (m, 8H, N(CH₂)₅), 1.25 – 1.18 (m, 4H, N(CH₂)₅). ¹³C{¹H} NMR (126 MHz, C₆D₆) δ 183.0 (t, ²J_{CP} = 3.7 Hz, C=Ir), 154.0 (vt, *J*_{CP} = 4.1 Hz, C-N(CH₂)₅, ArC), 150.3 (vt, *J*_{CP} = 9.3 Hz, ArC), 148.9 (vt, *J*_{CP} = 20.6 Hz, ArC), 143.0 (vt, *J*_{CP} = 17.5 Hz, ArC), 116.7 (s, ArCH), 105.1 (s, ArCH), 49.2 (s, N(CH₂)₂), 25.7 (vt, *J*_{CP} = 12.5 Hz, -CH(CH₃)₂), 25.4 (s, N(CH₂)₂), 24.4 (s, N(CH₂)₂), 19.9 (vt, *J* = 2.4 Hz, -CH(CH₃)₂), 19.5 (s, -CH(CH₃)₂). ³¹P{¹H} NMR (203 MHz, C₆D₆) δ 61.8 (s). Elemental Anal. Calcd. (%) for C₃₅H₅₂ClIrN₂OP₂: C 52.13; H 6.50; N 3.47. Found: C 52.36; H 6.71; N 3.09.

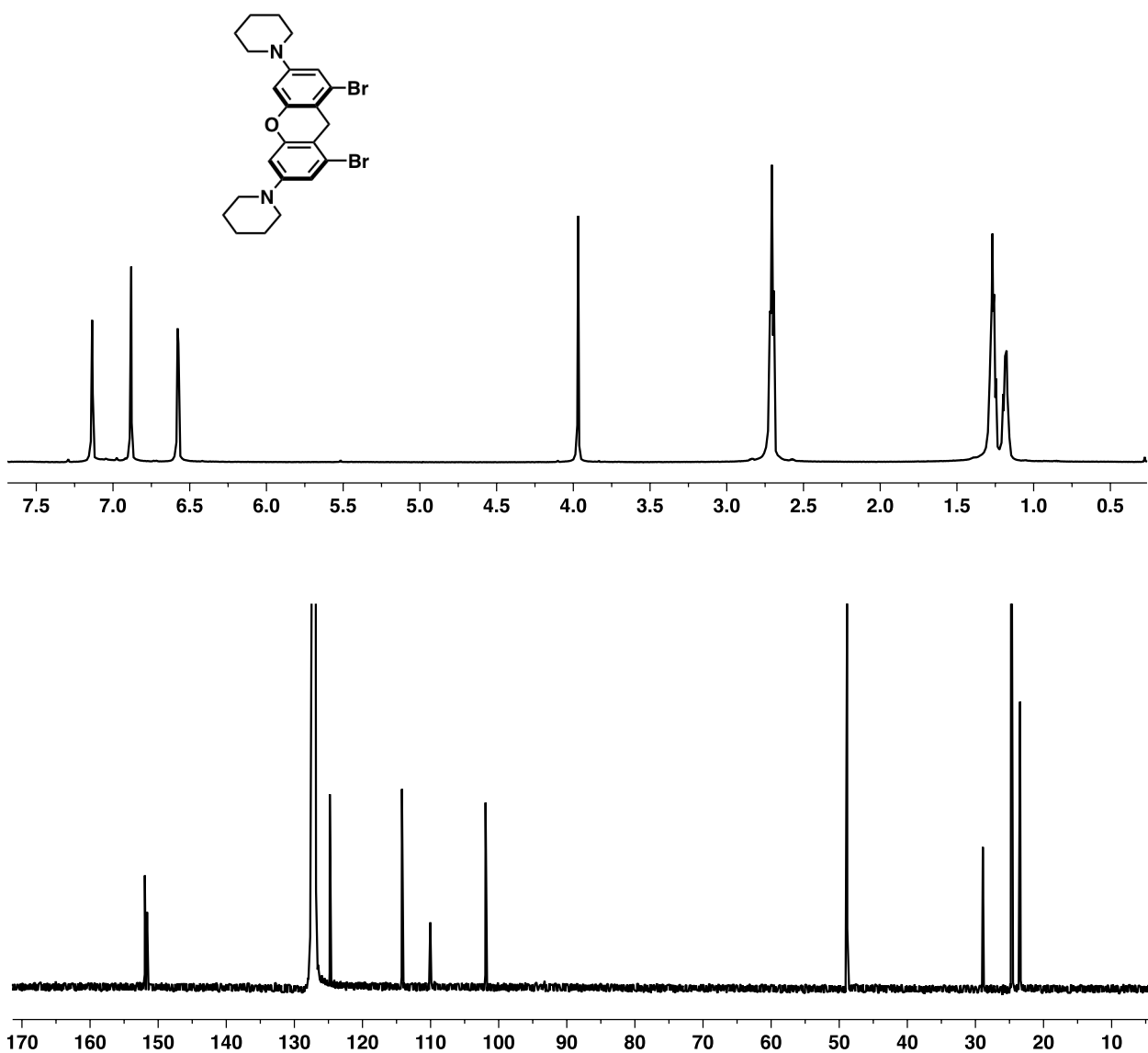


Figure S1. ^1H (top) and $^{13}\text{C}\{^1\text{H}\}$ (bottom) NMR spectra of 1,1'-(1,8-dibromo-9*H*-xanthene-3,6-diyl)dipiperidine in C_6D_6 .

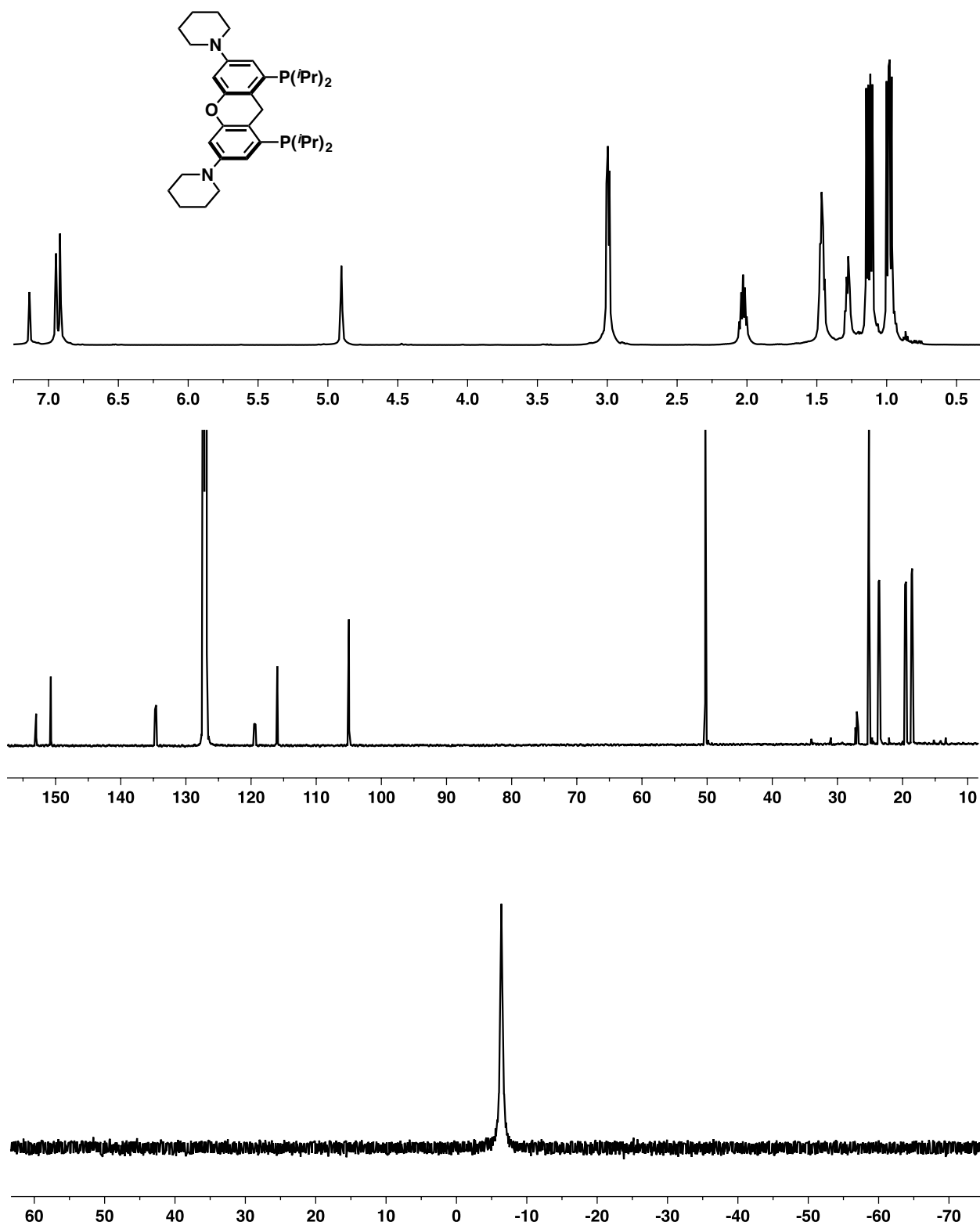


Figure S2. ^1H (top), $^{13}\text{C}\{\text{H}\}$ (middle), and $^{31}\text{P}\{\text{H}\}$ (bottom) NMR spectra of 1,1'-(1,8-bis(diisopropylphosphino)-9H-xanthene-3,6-diyl)dipiperidine in C_6D_6 .

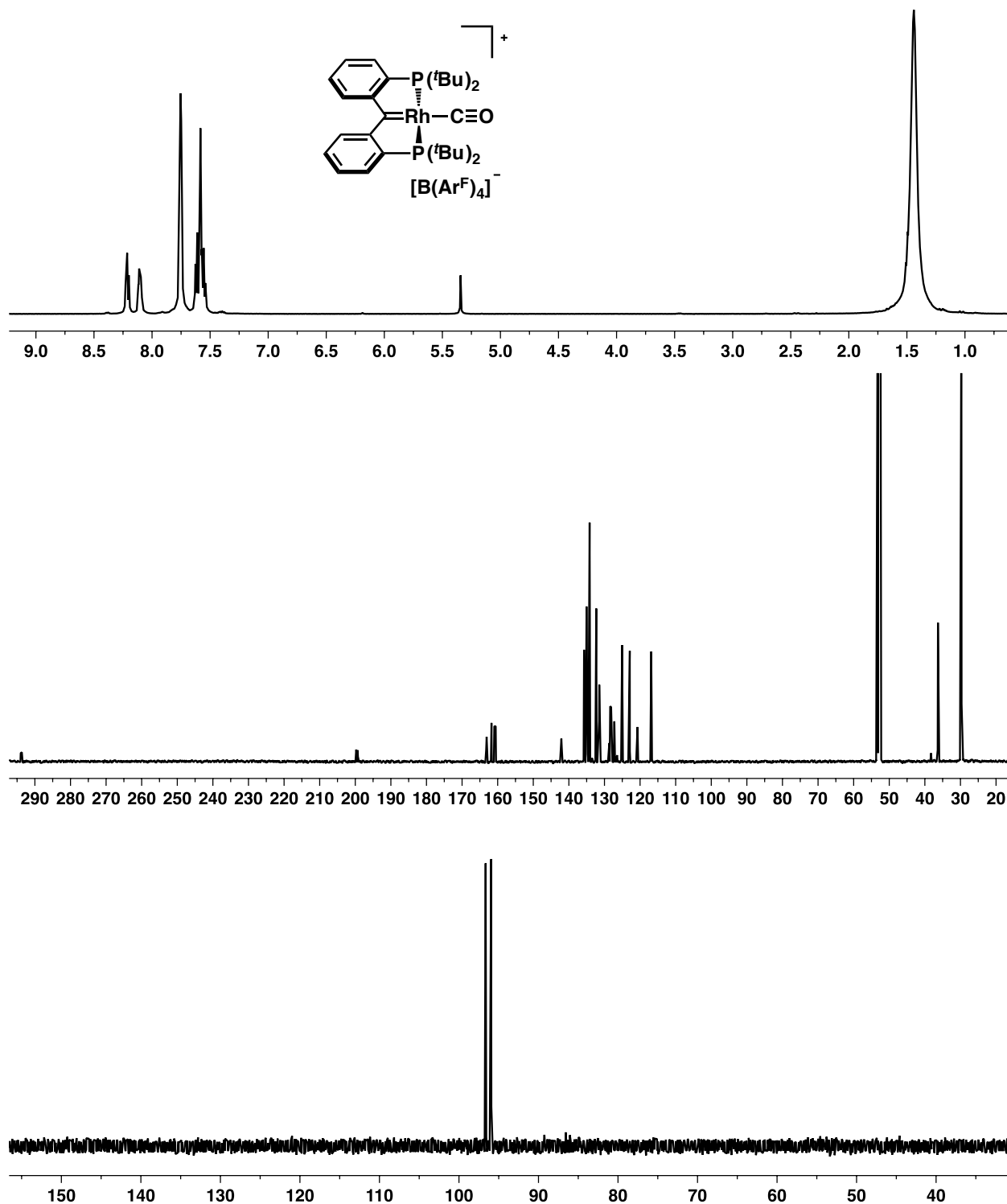


Figure S3. ^1H (top), $^{13}\text{C}\{^1\text{H}\}$ (middle), and $^{31}\text{P}\{^1\text{H}\}$ (bottom) NMR spectra of **1-CO** in CD_2Cl_2 .

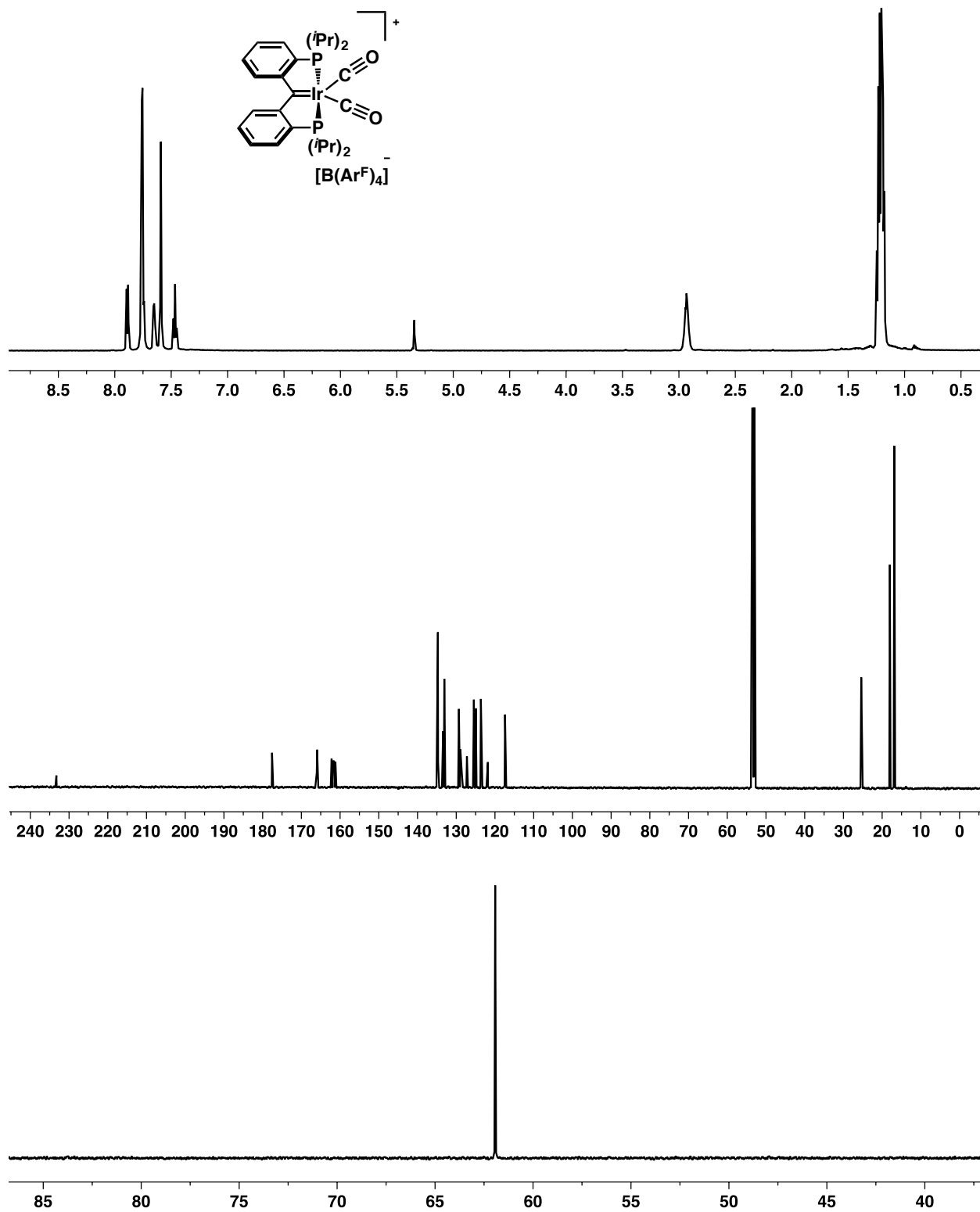


Figure S4. ^1H (top), $^{13}\text{C}\{^1\text{H}\}$ (middle), and $^{31}\text{P}\{^1\text{H}\}$ (bottom) NMR spectra of **2-iPr-(CO)₂** in CD_2Cl_2 .

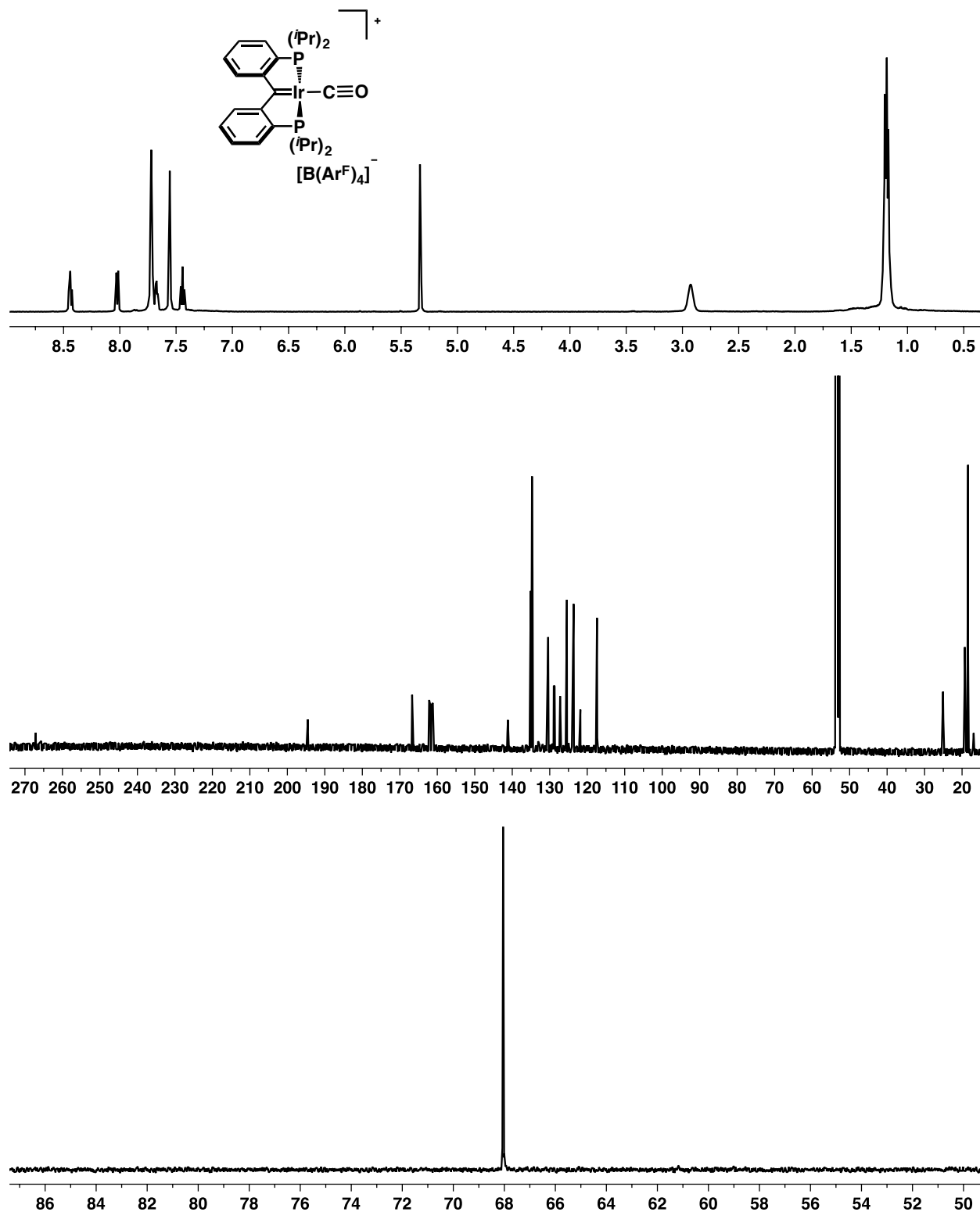


Figure S5. ^1H (top), $^{13}\text{C}\{\text{H}\}$ (middle), and $^{31}\text{P}\{\text{H}\}$ (bottom) NMR spectra of **2-iPr-CO** in CD_2Cl_2

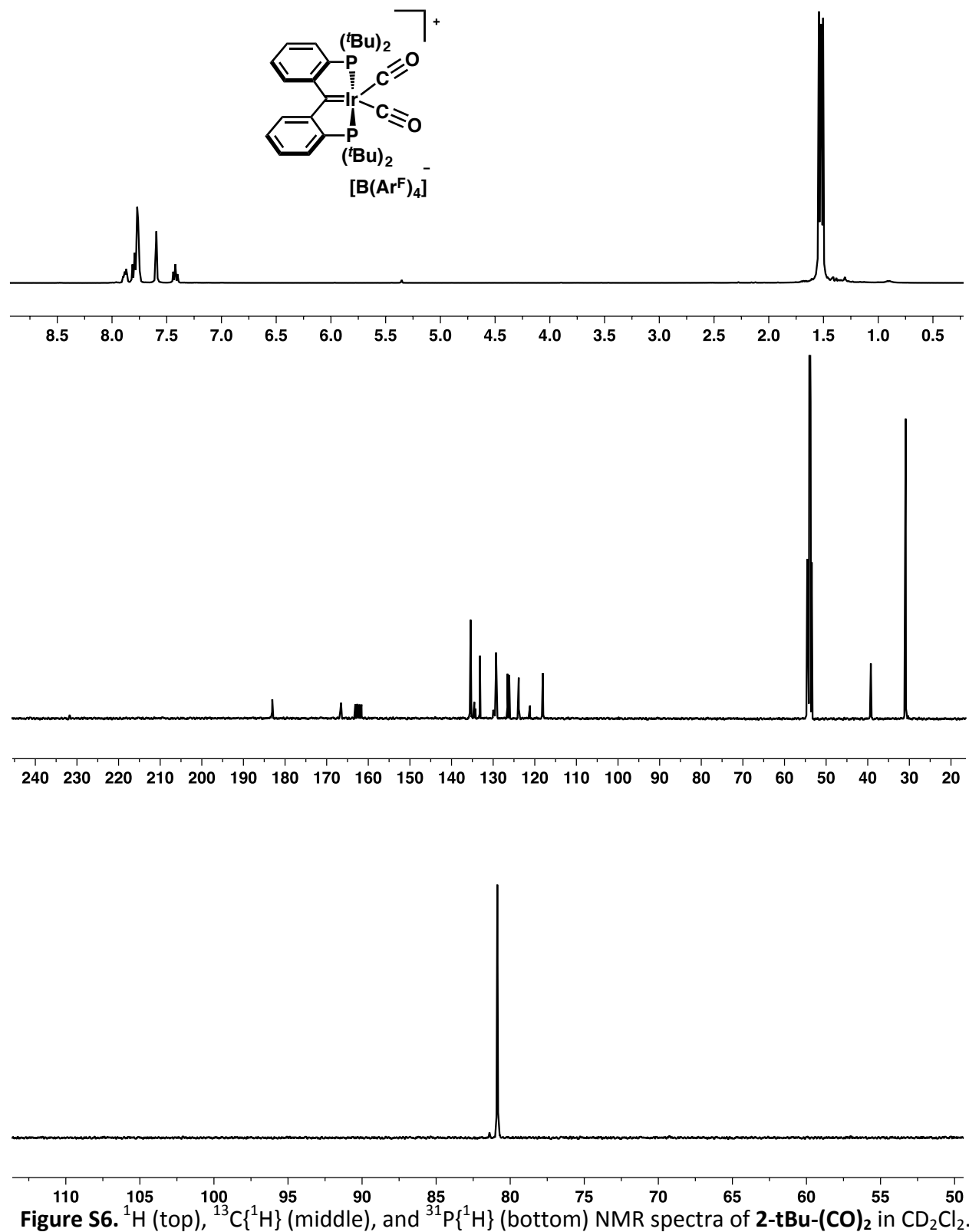


Figure S6. ¹H (top), ¹³C{¹H} (middle), and ³¹P{¹H} (bottom) NMR spectra of **2-tBu-(CO)₂** in CD₂Cl₂.

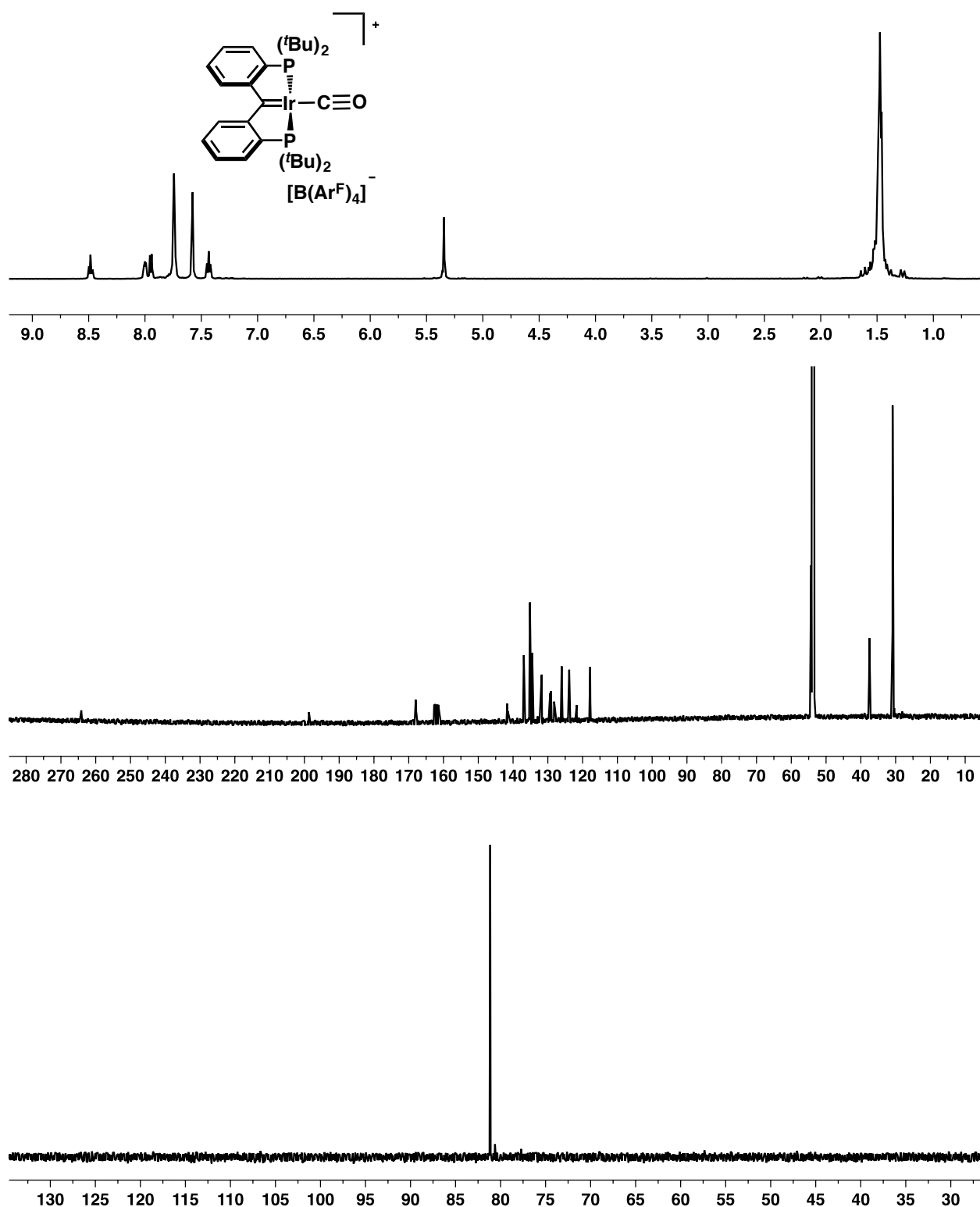


Figure S7. ^1H (top), $^{13}\text{C}\{^1\text{H}\}$ (middle), and $^{31}\text{P}\{^1\text{H}\}$ (bottom) NMR spectra of **2-tBu-CO** in CD_2Cl_2 .

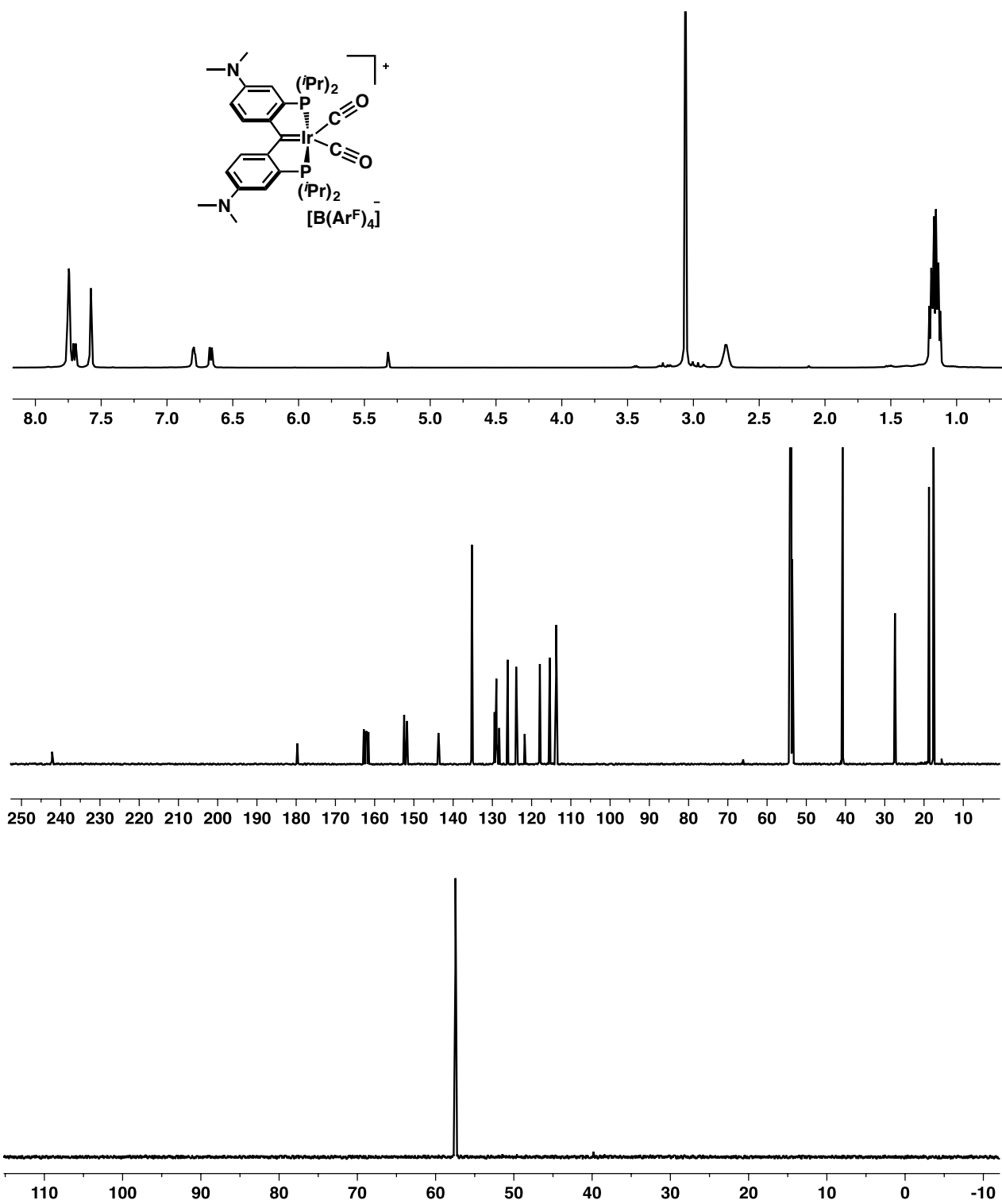


Figure S8. ^1H (top), $^{13}\text{C}\{^1\text{H}\}$ (middle), and $^{31}\text{P}\{^1\text{H}\}$ (bottom) NMR spectra of **3-(CO)₂** in CD_2Cl_2 .

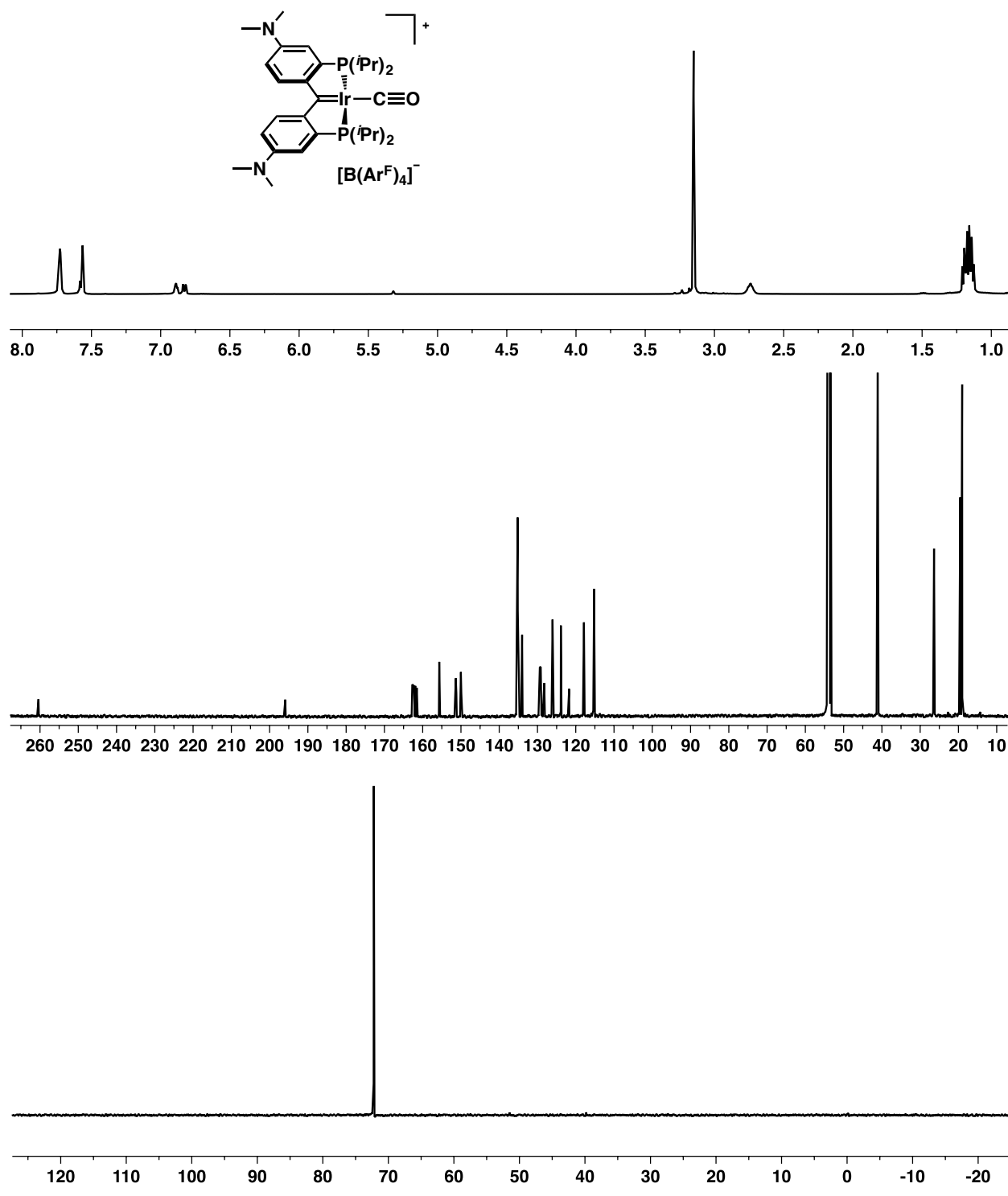


Figure S9. ^1H (top), $^{13}\text{C}\{^1\text{H}\}$ (middle), and $^{31}\text{P}\{^1\text{H}\}$ (bottom) NMR spectra of **3-CO** in CD_2Cl_2 .

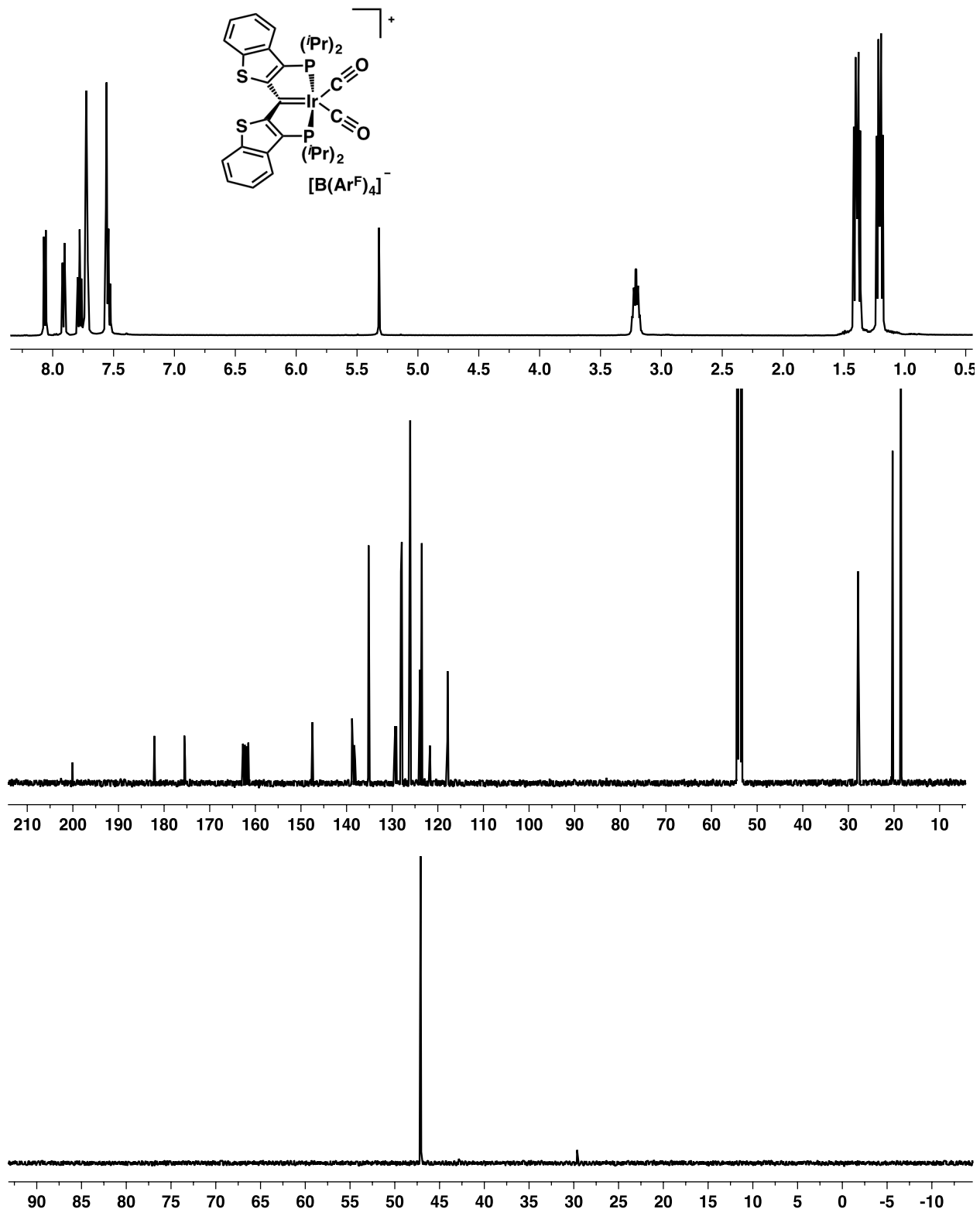


Figure S10. ^1H (top), $^{13}\text{C}\{^1\text{H}\}$ (middle), and $^{31}\text{P}\{^1\text{H}\}$ (bottom) NMR spectra of **4-(CO)₂** in CD_2Cl_2 .

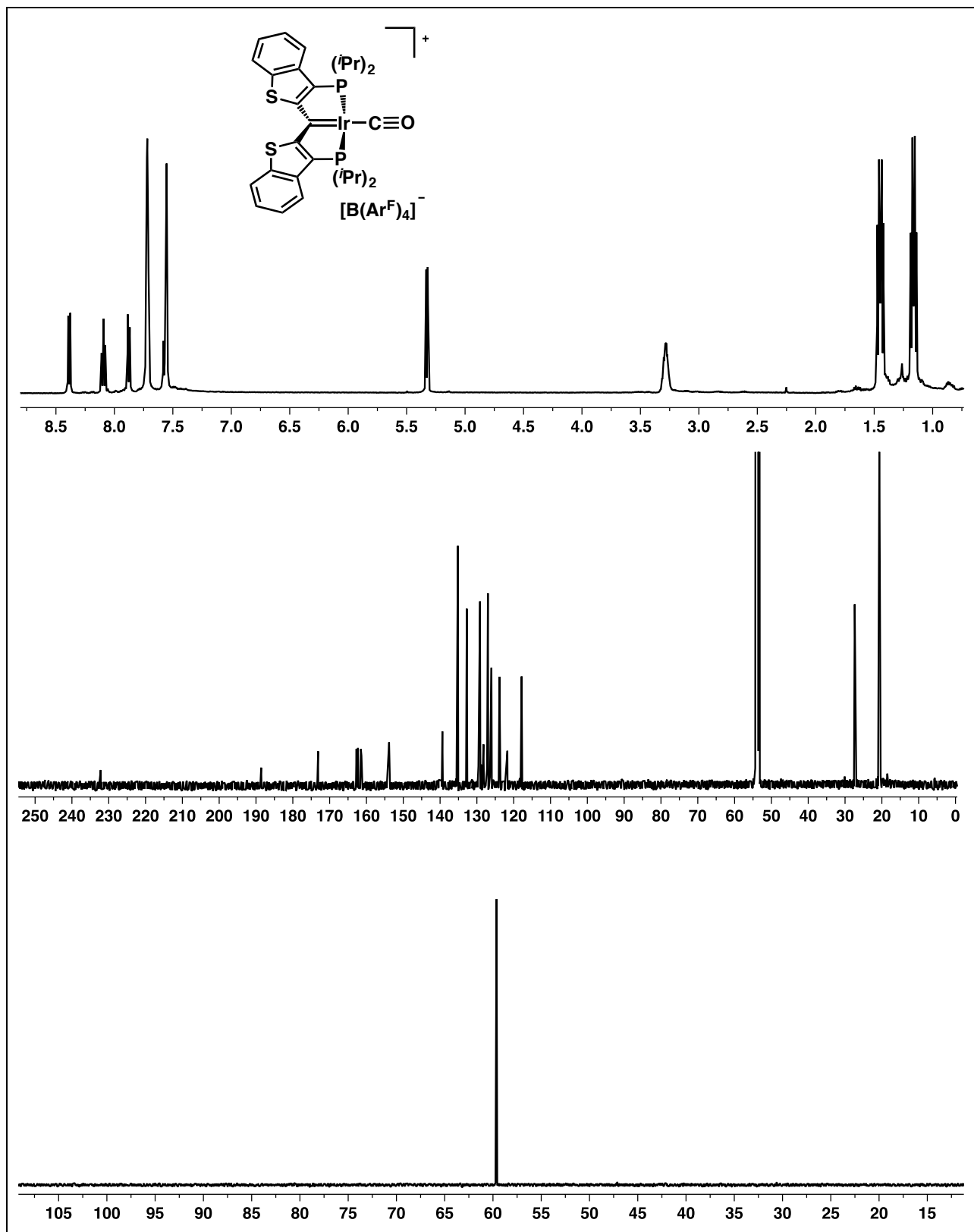


Figure S11. ^1H (top), $^{13}\text{C}\{^1\text{H}\}$ (middle), and $^{31}\text{P}\{^1\text{H}\}$ (bottom) NMR spectra of **4-CO** in CD_2Cl_2 .

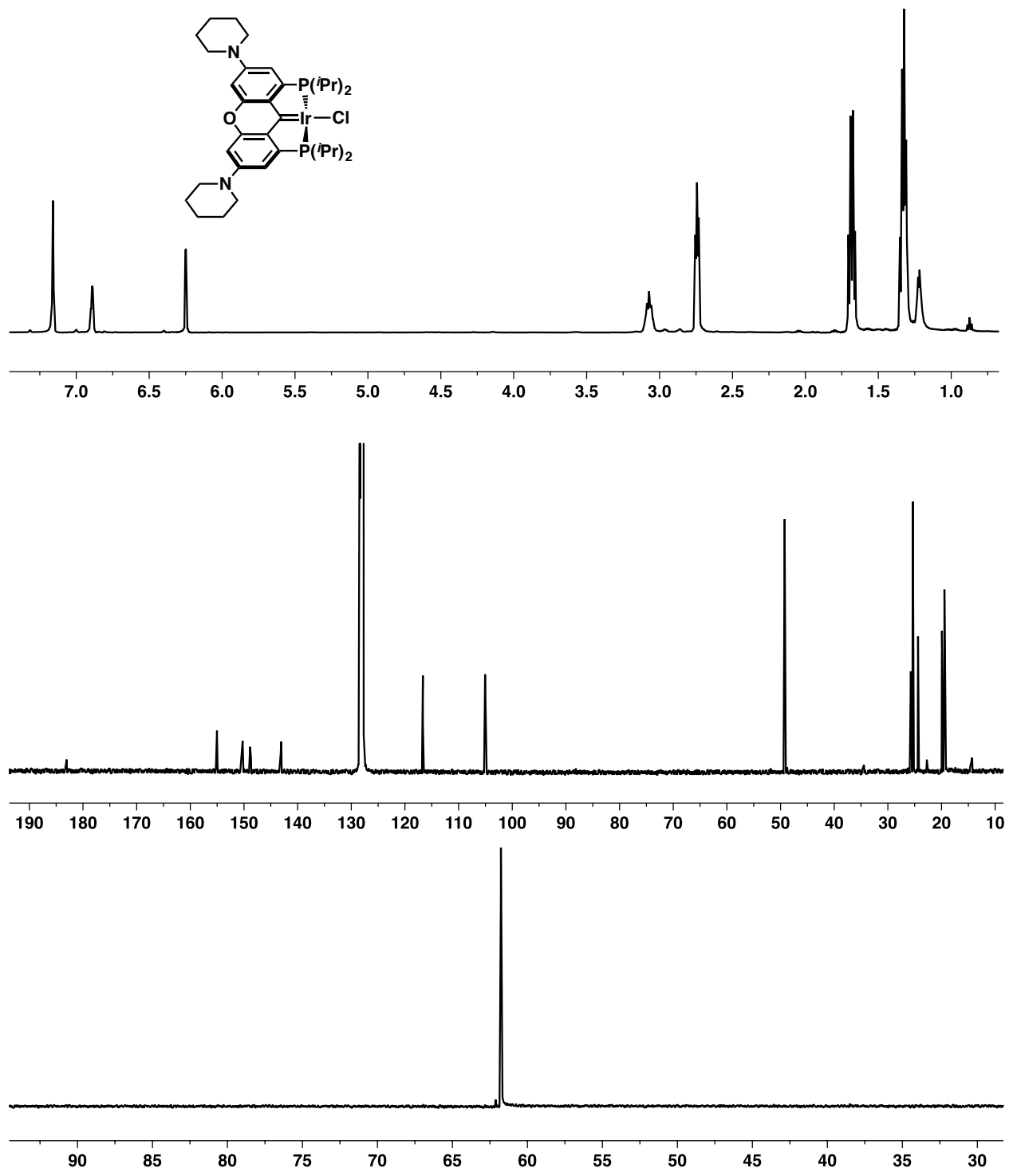


Figure S12. ^1H (top), $^{13}\text{C}\{^1\text{H}\}$ (middle), and $^{31}\text{P}\{^1\text{H}\}$ (bottom) NMR spectra of **5-Cl** in C_6D_6 .

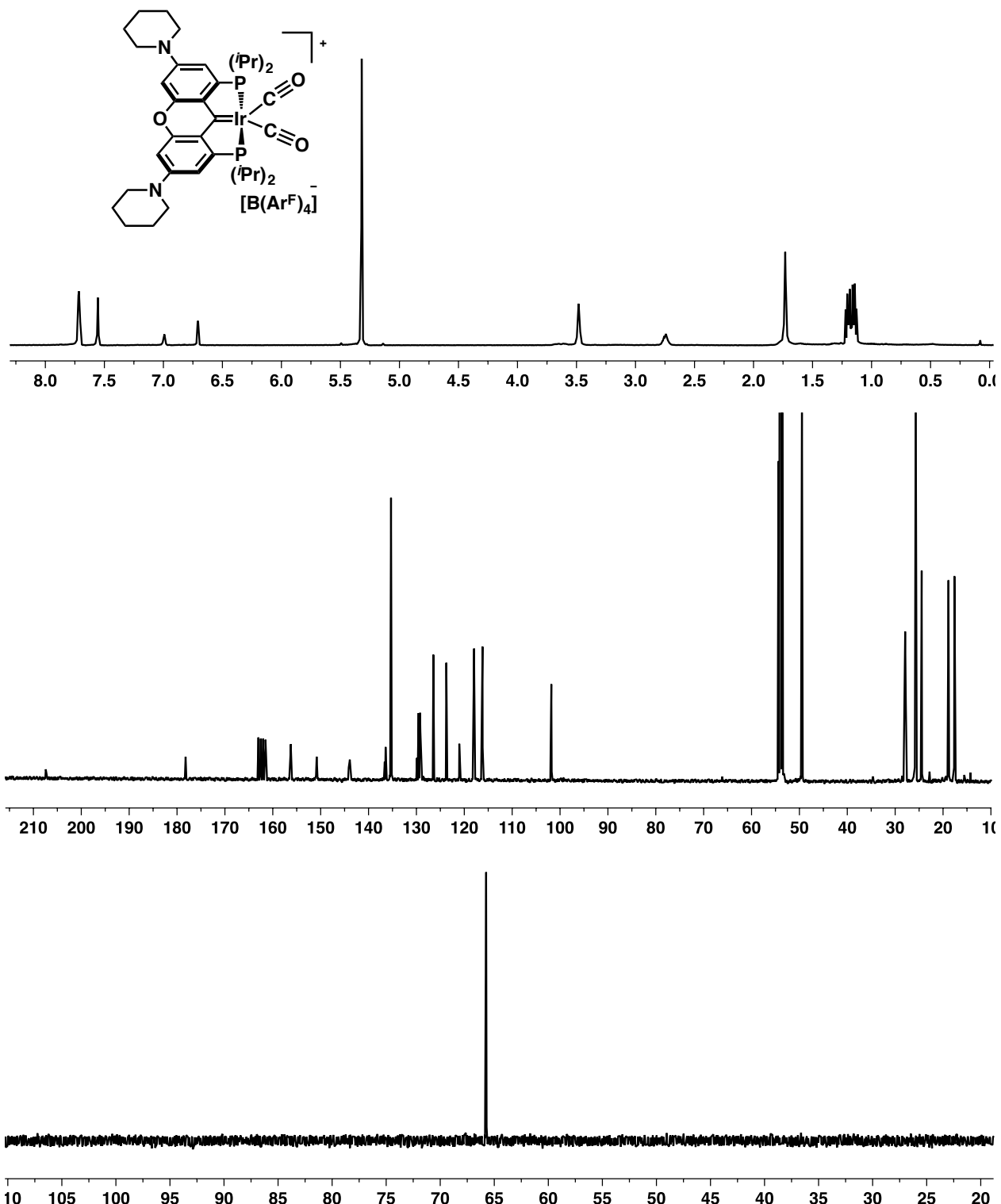


Figure S13. ^1H (top), $^{13}\text{C}\{^1\text{H}\}$ (middle), and $^{31}\text{P}\{^1\text{H}\}$ (bottom) NMR spectra of **5-(CO)₂** in CD_2Cl_2

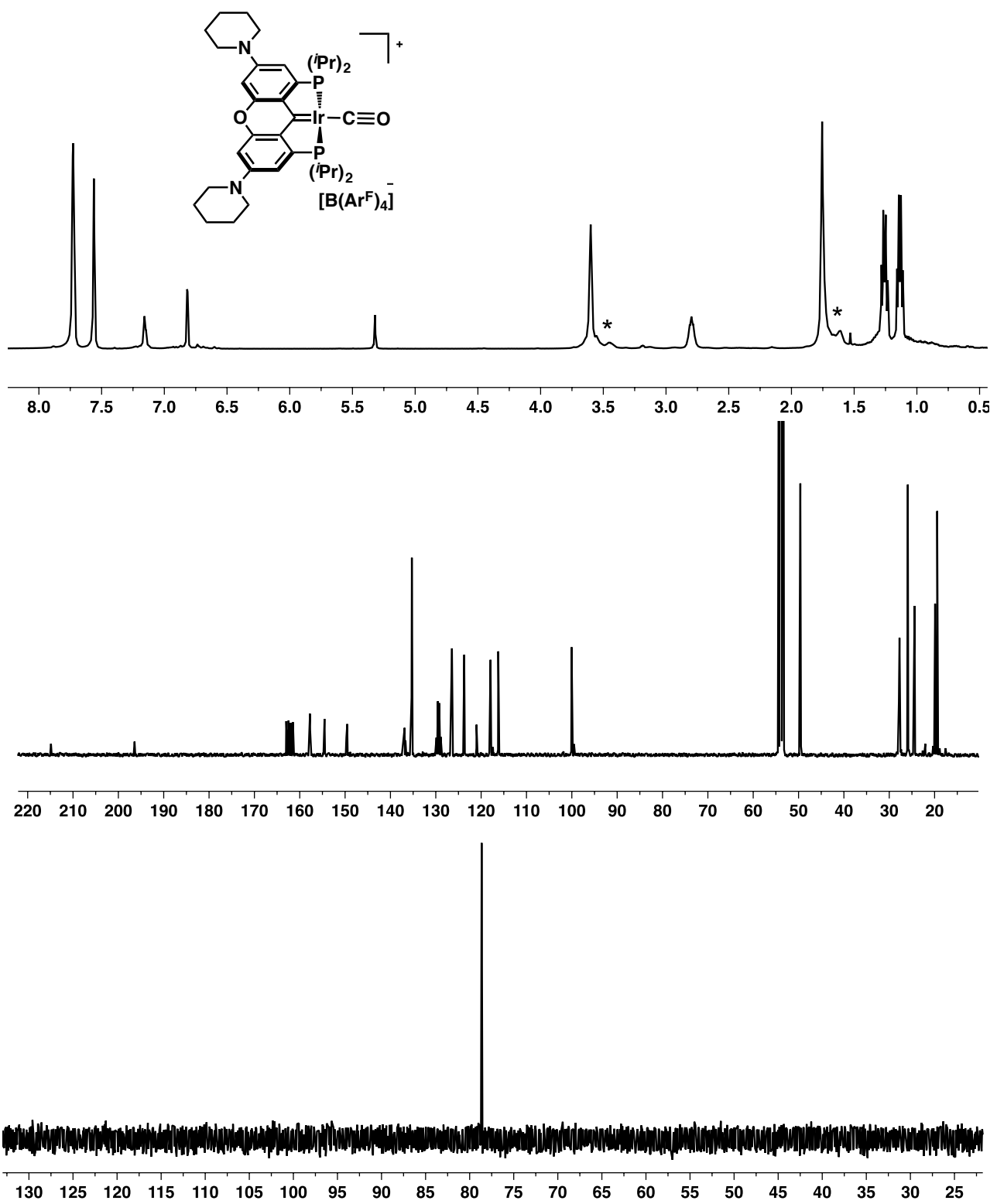


Figure S14. ^1H (top), $^{13}\text{C}\{^1\text{H}\}$ (middle), and $^{31}\text{P}\{^1\text{H}\}$ (bottom) NMR spectra of 5-CO in CD_2Cl_2 . *denotes unknown impurities.

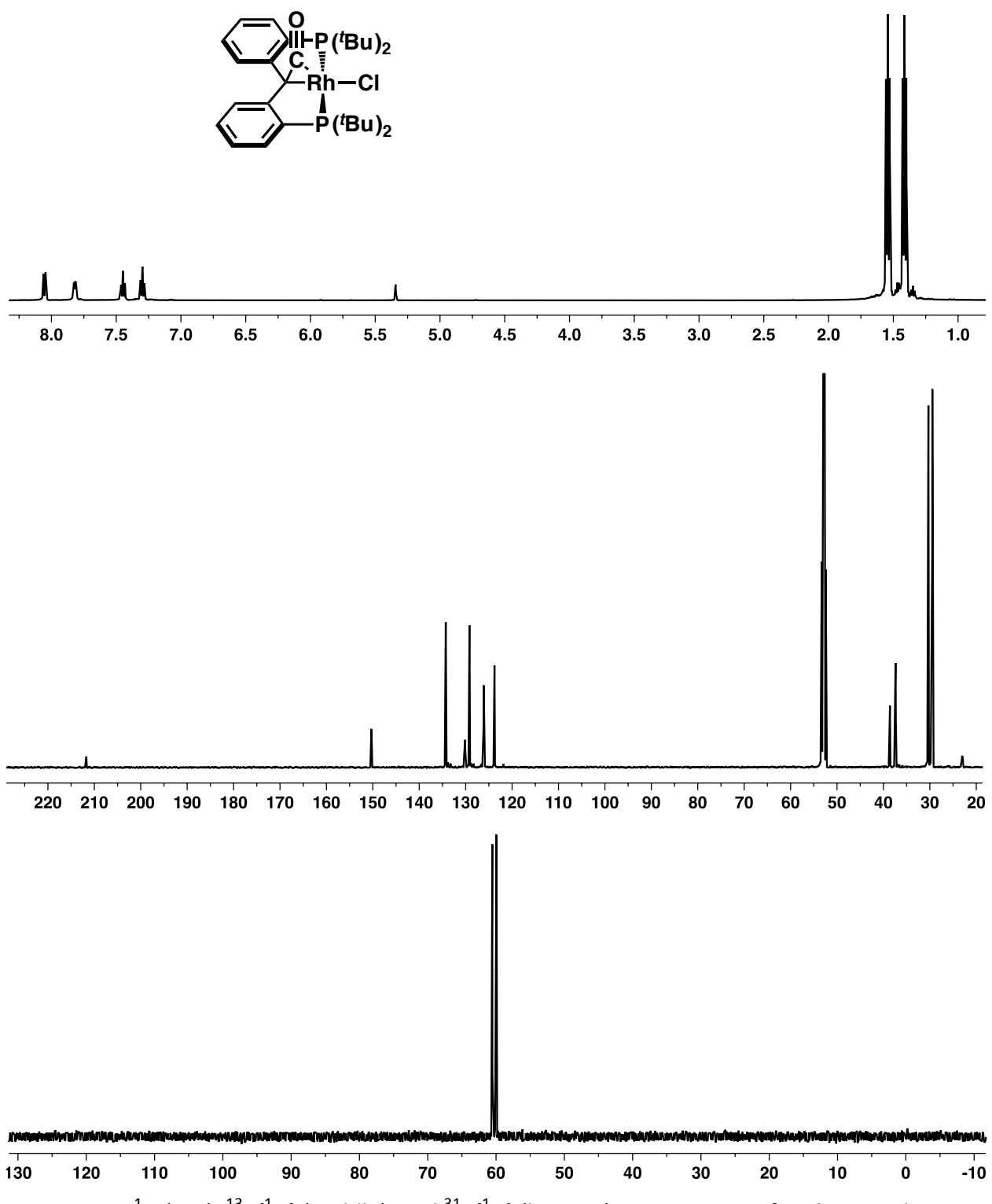


Figure S15. ^1H (top), $^{13}\text{C}\{^1\text{H}\}$ (middle), and $^{31}\text{P}\{^1\text{H}\}$ (bottom) NMR spectra of **6-Cl** in CD_2Cl_2 .

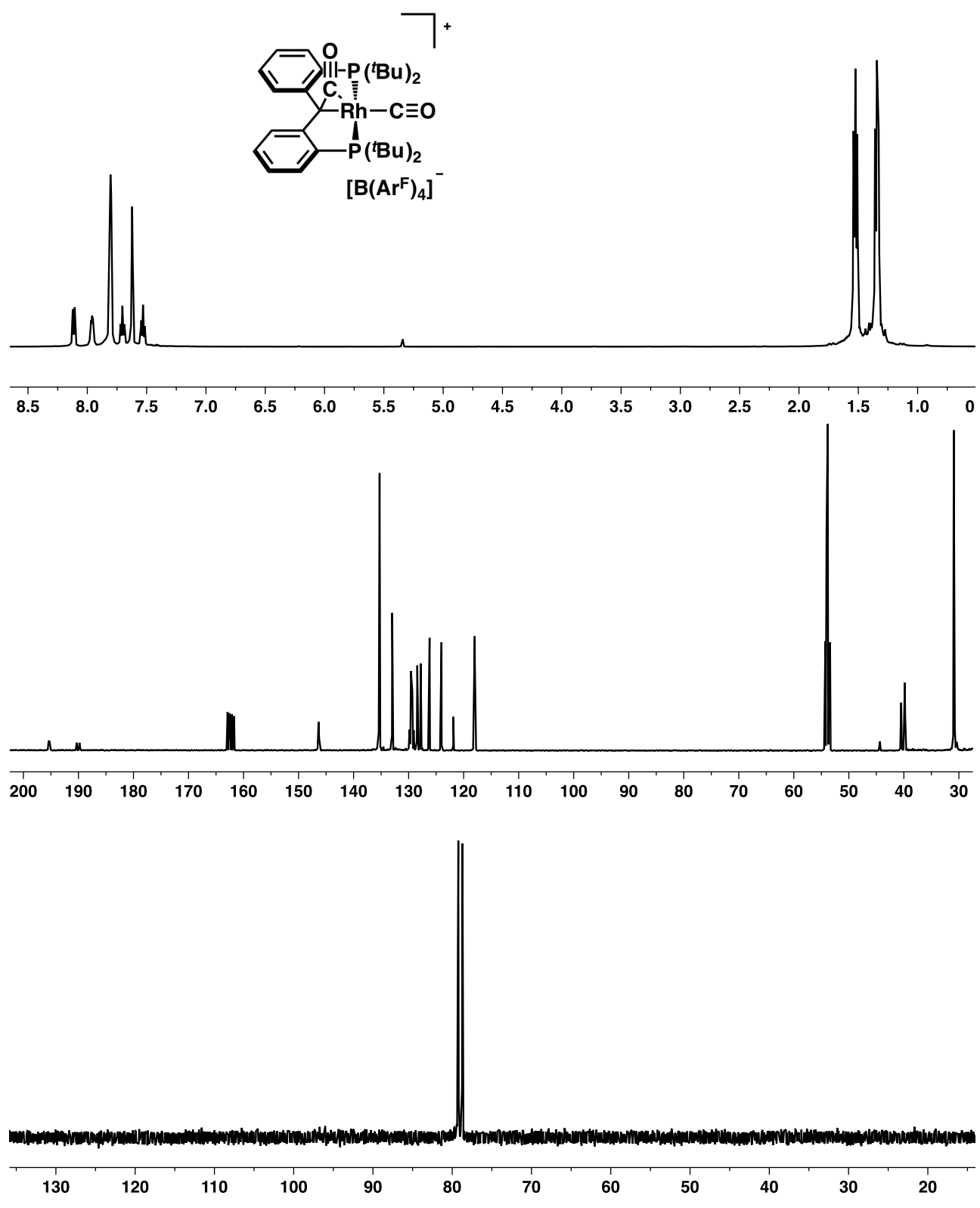


Figure S16. ^1H (top), $^{13}\text{C}\{^1\text{H}\}$ (middle), and $^{31}\text{P}\{^1\text{H}\}$ (bottom) NMR spectra of **6-CO** in CD_2Cl_2 .

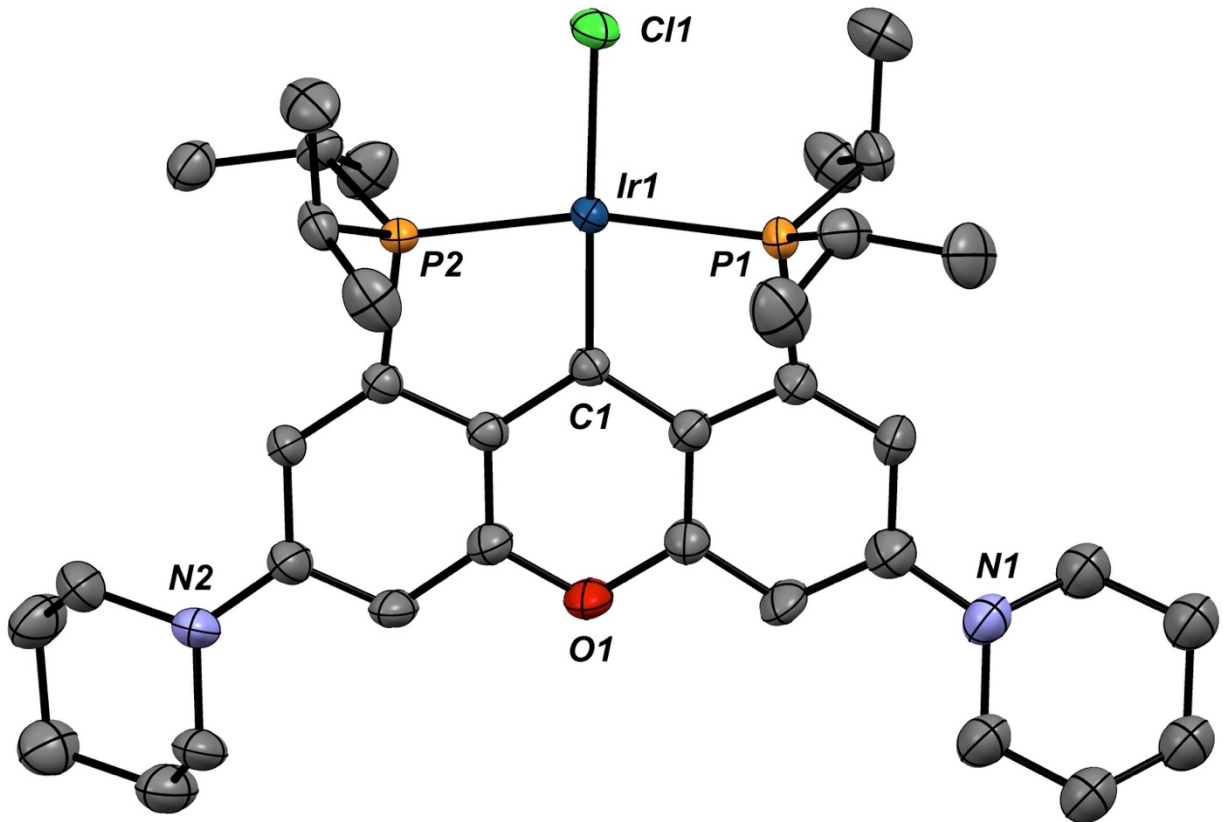


Figure S17. X-ray structure of **5-Cl** (thermal ellipsoids drawn to 50% probability level). Hydrogen atoms and the $B(Ar^F)_4$ counteranion are omitted for clarity. Selected bond distances (\AA): Ir1-C1 , 1.921(6); Ir1-Cl1 , 2.413(2); Ir1-P1 , 2.290(2); Ir1-P2 , 2.291(2). Selected bond angles ($^\circ$): P1-Ir1-P2 , 166.51(3); C1-Ir1-P1 , 83.4(3); C1-Ir1-Cl1 , 175.8(4); Cl1-Ir-P1 , 95.12(8).

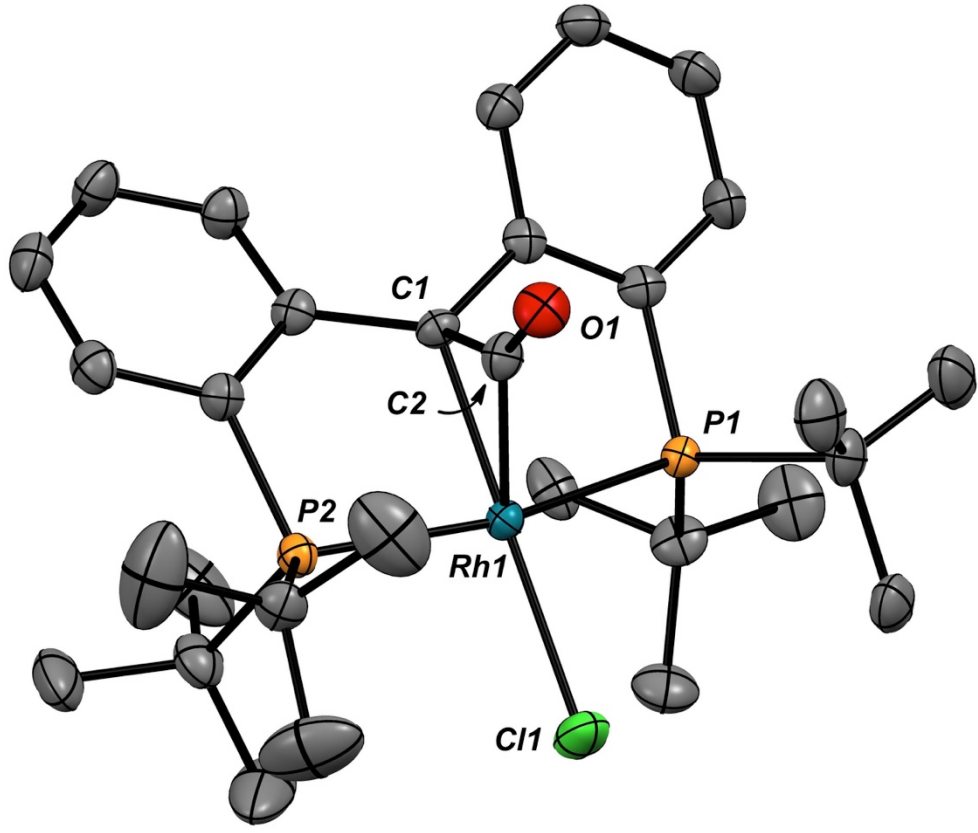
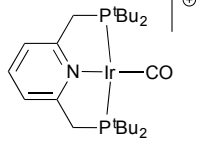
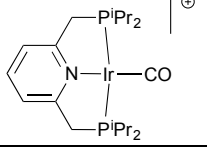
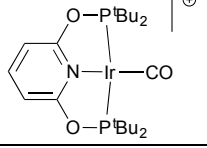
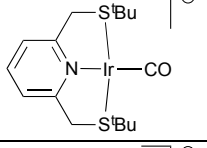
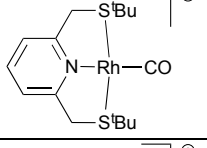
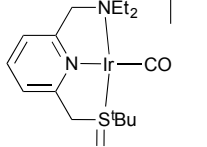
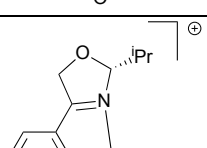
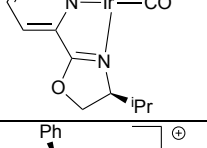
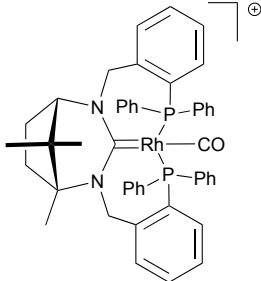


Figure S18. X-ray structure of **6-Cl** (thermal ellipsoids drawn to 50% probability level). Hydrogen atoms and the $B(\text{Ar}^F)_4$ counteranion are omitted for clarity. Selected bond distances (\AA): Rh1-C1, 2.116(3); Rh1-C2, 1.918(4); Rh1-Cl1, 2.396(1); Rh1-P1, 2.332(9); Rh1-P2, 2.331(9); C1-C2, 1.457(5); C2-O1, 1.192(5). Selected bond angles ($^\circ$): P1-Rh1-P2, 164.34(3); C1-Rh1-C2, 49.98(14); C1-Rh1-P1, 84.33(10); C1-C2-Rh1, 76.3(2); C1-C2-O1, 144.4(4); O1-C2-Rh1, 139.1(3); C2-C1-Rh1, 61.69(19).

Table S1. Iridium (I) monocarbonyl cations supported by pincer ligands

| Complex | IR (CO) cm ⁻¹ | Reference | Comments |
|---|---|-------------|---|
|  | 1962 1968 1964 | 1 2 3 | PF ₆ |
|  | 1970 | 2 | PF ₆ |
|  | 2010 | 4 | B(Ar _F) ₄ |
|  | 2000 (CH ₂ Cl ₂ soln) 1974 (solid) | 2 | BF ₄ |
|  | 2017(CH ₂ Cl ₂ soln) 1991 (solid) | 2 | BF ₄ |
|  | 1991 | 5 | BF ₄ M = Rh, 2009 |
|  | 1989 | 6 7 | PF ₆ R = Ph, 1996 M = Rh, 2001 |
|  | 1992 | 8 | BF ₄ |

| | | | |
|---|------|---|-----------------|
|  | 2009 | 9 | PF_6^- |
|---|------|---|-----------------|

1. Kloek, S. M.; Heinekey, D. M.; Goldberg, K. I., *Organometallics* **2006**, *25*, 3007-3011.
2. Klerman, Y.; Ben-Ari, E.; Diskin-Posner, Y.; Leitus, G.; Shimon, L. J. W.; Ben-David, Y.; Milstein, D., *Dalton Trans.* **2008**, 3226-3234.
3. Ben-Ari, E.; Cohen, R.; Gandelman, M.; Shimon, L. J. W.; Martin, J. M. L.; Milstein, D., *Organometallics* **2006**, *25*, 3190-3210.
4. Campos, J.; Kundu, S.; Pahls, D. R.; Brookhart, M.; Carmona, E.; Cundari, T. R., *J. Am. Chem. Soc.* **2013**, *135*, 1217-1220.
5. Schaub, T.; Radius, U.; Diskin-Posner, Y.; Leitus, G.; Shimon, L. J. W.; Milstein, D., *Organometallics* **2008**, *27*, 1892-1901.
6. Díez, J.; Gamasa, M. P.; Gimeno, J.; Paredes, P., *Organometallics* **2005**, *24*, 1799-1802.
7. Cuervo, D.; Díez, J.; Gamasa, M. P.; Gimeno, J.; Paredes, P., *Eur. J. Inorg. Chem.* **2006**, *2006*, 599-608.
8. Valyaev, D. A.; Filippov, O. A.; Lugan, N.; Lavigne, G.; Ustyynyuk, N. A., *Angew. Chem. Int. Ed.* **2015**, *54*, 6315-6319.
9. Newman, P. D.; Cavell, K. J.; Kariuki, B. M., *Dalton Trans.* **2012**, *41*, 12395-12407.

Table S2. Data collection and structure refinement details for **1-CO**, **iPr-2-(CO)₂** and **3-CO**.

| | 1-CO | iPr-2-(CO)₂ | 3-CO |
|---|---|--|---|
| formula | C ₃₂ H ₁₂ BF ₂₄ , C ₃₀ H ₄₄ OP ₂ Rh | C ₃₂ H ₁₂ BF ₂₄ , C ₂₇ H ₃₆ IrO ₂ P ₂ | C ₃₂ H ₁₂ BF ₂₄ , C ₃₀ H ₄₆ IrN ₂ OP ₂ |
| <i>fw</i> | 1448.72 | 1509.92 | 1568.05 |
| crystal system | Triclinic | Monoclinic | Monoclinic |
| space group | P-1 | P21/c | P21/c |
| <i>a</i> (Å) | 12.5448(4) | 14.9490(4) | 10.214 |
| <i>b</i> (Å) | 13.0536(3) | 25.1541(8) | 24.803 |
| <i>c</i> (Å) | 21.3007(6) | 19.1154(5) | 26.256 |
| α (deg) | 76.054(2) | 90.00 | 90 |
| β (deg) | 89.231(2) | 120.2530(10) | 98.34 |
| γ (deg) | 88.112(2) | 90.00 | 90 |
| <i>V</i> (Å³) | 3383.38(17) | 6209.0(3) | 6581.3 |
| <i>Z</i> | 2 | 4 | 4 |
| <i>T</i> (K) | 293(2) | 173(2) | 293(2) |
| Wavelength (Å) | 1.54178 | 0.71073 | 0.7107 |
| ρ_{calcd} (g·cm⁻³) | 1.422 | 1.615 | 1.583 |
| <i>F</i>(000) | 1464 | 2984 | 3120 |
| μ (mm⁻¹) | 3.427 | 2.315 | 2.187 |
| crystal size, mm³ | 0.20×0.20×0.20 | 0.07×0.06×0.05 | 0.2×0.04×0.04 |
| transmission factors | 0.5631 – 0.7823 | 0.8547 – 0.8930 | 0.734 – 0.872 |
| ϑ range (deg) | 2.137 – 67.497 | 2.30 – 26.00 | 1.135 – 27.463 |
| data/restraints/param | 11734/481/980 | 11820/0/802 | 14914/396/1020 |
| GOF | 1.015 | 1.136 | 1.192 |
| R₁ [I > 2σ(I)] | 0.1175 | 0.0632 | 0.0737 |
| wR₂ [all data] | 0.3316 | 0.1361 | 0.2188 |
| residual density, e/Å³ | 2.982 and -0.802 | 0.998 and -0.802 | 1.335 and -1.542 |

Table S3. Data collection and structure refinement details for **4-CO**, **5-Cl**, **6-Cl** and **6-CO**.

| | 4-CO | 5-Cl | 6-Cl | 6-CO |
|--|--|--|--|--|
| formula | C ₃₁ H ₃₆ IrO ₂ P ₂ S ₂ ,C ₃₂ H ₁₂ BF ₂₄ | C ₃₆ H ₅₄ Cl ₃ IrN ₂ OP ₂ | C ₃₀ H ₄₄ ClOP ₂ Rh | C ₃₀ H ₄₄ ClOP ₂ Rh |
| fw | 1622.08 | 891.30 | 620.95 | 620.95 |
| crystal system | Triclinic | Orthorhombic | Monoclinic | Monoclinic |
| space group | P -1 | Pna21 | P21/n | P21/n |
| a (Å) | 11.4951(3) | 11.3542(2) | 9.2218(3) | 9.2218(3) |
| b (Å) | 17.2586(3) | 28.9341(3) | 22.3093(6) | 22.3093(6) |
| c (Å) | 18.9432(5) | 11.62320(10) | 14.3694(4) | 14.3694(4) |
| α (deg) | 68.300(3) | 90 | 90 | 90 |
| β (deg) | 85.1920(10) | 90 | 95.2020(10) | 95.2020(10) |
| γ (deg) | 90.094(2) | 90 | 90 | 90 |
| V(Å³) | 3477.35(14) | 3818.50(8) | 2944.07(15) | 2944.07(15) |
| Z | 2 | 4 | 4 | 4 |
| T (K) | 173(2) | 173(2) | 293(2) | 293(2) |
| Wavelength (Å) | 0.71073 | 1.54178 | 1.54178 | 1.54178 |
| ρ_{calcd} (g·cm⁻³) | 1.549 | 1.550 | 1.401 | 1.401 |
| F(000) | 1604 | 1800 | 1296 | 1296 |
| μ (mm⁻¹) | 2.131 | 9.721 | 6.702 | 6.702 |
| crystal size, mm³ | 0.06×0.04×0.02 | 0.10×0.04×0.01 | 0.35×0.31×0.20 | 0.35×0.31×0.20 |
| transmission factors | 0.8828 – 0.9586 | 0.4088 – 0.5864 | 0.5485 – 0.7536 | 0.5485 – 0.7536 |
| θ range (deg) | 2.02 – 26.00 | 3.055 – 67.488 | 3.669 – 66.999 | 3.669 – 66.999 |
| data/restraints/param | 13564/0/856 | 5882/657/470 | 5164/72/378 | 5164/72/378 |
| GOF | 1.049 | 1.006 | 1.021 | 1.021 |
| R₁ [I > 2σ(I)] | 0.0585 | 0.0318 | 0.0417 | 0.0417 |
| wR₂ [all data] | 0.1426 | 0.0670 | 0.1092 | 0.1092 |
| residual density, e/Å³ | 1.560 and -0.880 | 0.732 and -0.452 | 1.613 and -0.706 | 1.613 and -0.706 |

References

- (1) Herde, J. L.; Lambert, J. C.; Senoff, C. V.; Cushing, M. A. In *Inorganic Syntheses*; Parshall, G. W., Ed.; John Wiley & Sons, Inc.: Hoboken, NJ, USA, 2007; pp 18–20.
- (2) Sugawara, S.; Abe, M.; Fujiwara, Y.; Wakioka, M.; Ozawa, F.; Yamamoto, Y. *Eur. J. Inorg. Chem.* **2015**, 2015 (3), 534–541.
- (3) Brookhart, M.; Grant, B.; Volpe, A. F. *Organometallics* **1992**, 11 (11), 3920–3922.